Advanced terahertz electric near-field measurements at sub-wavelength diameter metallic apertures

A. J. L. Adam,[1], J. M. Brok,[1], M. A. Seo[2], K. J. Ahn,[2], D. S. Kim,[2*]
J. H. Kang,[3], Q. H. Park,[3], M. Nagel,[4], P. C. M. Planken[1,5*]

[1]*Faculty of Applied Physics, Department of Imaging Science and Technology, Lorentzweg 1, 2628 CJ Delft, The Netherlands*
[2]*School of Physics and Astronomy, Seoul National University, Seoul 151-747, Korea*
[3]*Department of Physics, Korea University, Seoul 136-701, Korea*
[4] *Institut für Halbleitertechnik, RWTH Aachen University, Sommerfeldstr. 24 52074 Aachen, Germany*
[5] *FOM Institute for Plasma Physics 'Rijnhuizen', Edisonbaan 14, 3439 MN, Nieuwegein The Netherlands*
[*] *Corresponding author: p.c.m.planken@tudelft.nl; denny@snu.ac.kr*

Abstract: Using terahertz-light excitation, we have measured with sub-wavelength spatial, and sub-cycle temporal resolution the time- and frequency-dependent electric-field and surface-charge density in the vicinity of small metallic holes. In addition to a singularity like concentration of the electric field near the hole edges, we observe, that holes can act as differential operators whose near-field output is the time-derivative of the incident electric field. Our results confirm the well-known predictions made by Bouwkamp, Philips Res. Rep. **5**, 321-332 (1950), and reveal, with unprecedented detail, what physically happens when light passes through a small hole.

OCIS codes: (180.4243) Near-field microscopy; (050.1220) Apertures; (300.6495) Spectroscopy, Terahertz;

References and links

1. T. W. Ebbesen, H. J. Lezec, H. F. Ghaemi, T. Thio, and P. A. Wolff, "Extraordinary optical transmission through sub-wavelength hole arrays," Nature (London) **391**, 667-669 (1998)
2. T. Matsui, A. Agrawal, A. Nahata, and Z. V. Vardeny, "Transmission resonances through aperiodic arrays of subwavelength apertures," Nature (London) **447**, 517-521 (2007)
3. L. Novotny, D. W. Pohl, B. Hecht, "Scanning near-field optical probe with ultrasmall spot size," Opt. Lett. **20**, 970-972 (1995)
4. E. Betzig, J. K. Trautman, "Single Molecules Observed by Near-Field Scanning Optical Microscopy," Science **257**, 189-195 (1992)
5. B. Hecht, B. Sick, U. P. Wild, V. Deckert, R. Zenobi, O. J. F. Martin, D. W. Pohl, "Scanning near-field optical microscopy with aperture probes: Fundamentals and applications," J. Chem. Phys. **112**, 7761-7774 (2000)
6. J. T. Bahns, F. Yan, D. Qiu, R. Wang, L. Chen, "Hole-enhanced Raman scattering," Appl. Spectrosc. **60**, 989-993 (2006)
7. A. G. Brolo, E. Arctander, R. Gordon, B. Leathem, K. L. Kavanagh, "Nanohole-enhanced Raman scattering," Nano Lett. **4**, 2015-2018 (2004)
8. A. Degiron, H. J. Lezec, N. Yamamoto, T. W. Ebbesen, "Optical transmission properties of a single subwavelength aperture in a real metal," Opt. Commun. **239**, 61-66 (2004)
9. R. S. Decca, H. D. Drew, K. L. Empson, "Investigation of the electric-field distribution at the subwavelength aperture of a near-field scanning optical microscope," Appl. Phys. Lett. **70**, 1932-1934 (1997)

#94461 - $15.00 USD Received 1 Apr 2008; revised 25 Apr 2008; accepted 25 Apr 2008; published 6 May 2008

10. C. Genet, T. W. Ebbesen, "Light in tiny holes," Nature (London) **445**, 39-46 (2007)
11. E. Betzig, R. J. Chichester, "Single molecules observed by near-field scanning optical microscopy," Science **262**, 1422-1425 (1993)
12. J. A. Veerman, M. F. Garcia-Parajo, L. Kuipers, N. F. Van Hulst, "Single molecule mapping of the optical field distribution of probes for near-field microscopy," J. Microsc. **194**, 477-482 (1999)
13. A. Drezet, S. Huant, J. C. Woehl, "In situ characterization of optical tips using single fluorescent nanobeads," J. Lumin. **107**, 176-181 (2004)
14. H. A. Bethe, "Theory of diffraction by small holes," Phys. Rev. **66**, 163-182 (1944)
15. C. J. Bouwkamp, "On the diffraction of electromagnetic waves by circular disks and apertures," Philips Res. Rep. **5**, 401-422 (1950)
16. C. J. Bouwkamp, "On Bethe's theory of diffraction by small holes," Philips Res. Rep. **5**, 321-332 (1950)
17. A. Agrawal, H. Cao, and A. Nahata,"Time-domain analysis of enhanced transmission through a single subwavelength aperture," Opt. Express **13**, 3535-3542 (2005)
18. A. Agrawal and A. Nahata, "Time-domain radiative properties of a single subwavelength aperture surrounded by an exit side surface corrugation," Opt. Express **14**, 1973-1981 (2006)
19. M. van Exter, D. R. Grischkowsky, "Characterization of an Optoelectronic Terahertz Beam System," IEEE Trans. Microwave Theory Tech. **38**, 1684-1691 (1990)
20. G. Zhao, R. N. Schouten, N. van der Valk, W. Th. Wenckebach, and P. C. M. Planken, "Design and performance of a THz emission and detection setup based on a semi-insulating GaAs emitter," Rev. Sci. Instrum. **73**, 1715-1719 (2002)
21. N. C. J. van der Valk, P. C. M. Planken, "Electro-optic detection of sub-wavelength terahertz spot sizes in the near-field of a metal tip," Appl. Phys. Lett. **81**, 1558-1560 (2002)
22. M. A. Seo et al, "Fourier-transform terahertz near-field imaging of one-dimensional slit arrays: mapping of electric-field-, magnetic-field-, and Poynting vectors," Opt. Express **15**, 11781-11789 (2007)
23. F. J. García de Abajo, J. J. Sáenz, I. Campillo, and J. S. Dolado, "Site and lattice resonances in metallic hole arrays," Opt. Express **14**, 7-18 (2006)
24. R. Gordon, A. G. Brolo, "Increased cut-off wavelength for a subwavelength hole in a real metal," Opt. Express **13**, 1933-1938 (2005)
25. F. J. García de Abajo, "Light transmission through a single cylindrical hole in a metallic film," Opt. Express **10**, 1475-1484 (2002)
26. T. Thio et al., "Giant optical transmission of sub-wavelength apertures: physics and applications," Nanotechnology **13**, 429-432 (2002)
27. O. Mitrofanov et al., "Terahertz pulse propagation through small apertures," Appl. Phys. Lett. **79**, 907-909 (2001)
28. G. A. Massey, J. A. Davis, S. M. Katnik, and E. Ornon, "Subwavelength resolution far-infrared microscopy," Appl. Opt. **24**, 1498-1501 (1985)
29. E. F. Barnett and J. K. Hunton, "A precision directional coupler using multi-hole coupling," Hewlett Packard Journal, **3** (No. 7-8) (1952).
30. J. F. Nye, W. Liang, and G. Hygate, "Mapping a diffraction field close to an obstacle," IEEE Trans. Electromagn. Compat. **37**, 288-292 (1995).
31. J. F. Nye and W. Liang, "Superposition of the diffraction fields of apertures: an experimental test," Proc. R. Soc. Lond. A **453**, 1963-1974 (1997).

1. Introduction

How does light diffract from a small hole? In nanophotonics this question is extremely relevant.[1, 2, 3] The very extent of the electromagnetic field near a hole, for instance, can determine the spatial resolution in near-field microscopy.[4] Knowledge of the near-field optical spectrum, which can be very different from the far-field optical spectrum, is very important for any spectroscopic measurement.[5] In addition, local field enhancements, caused by charge accumulation near sharp sub-wavelength features such as the hole edges, could have a dramatic influence on the efficiency of various non-linear optical processes, such as Raman scattering.[6, 7] Past reports on near-field measurements on small holes showed evidence of light concentration near the edges.[8, 9, 10, 11, 12, 13] However, the exact nature of the near electric-field of sub-wavelength holes is still largely unknown since adequate experimental techniques to measure the near-field of a sub-wavelength hole are lacking. Numerical and analytical *calculations* can make predictions about the near-field of a hole but are not without problems. Every theoretical model has to include some simplifying assumptions, so that differences with the real-world behavior of fields are unavoidable. For example, the most widely

#94461 - $15.00 USD Received 1 Apr 2008; revised 25 Apr 2008; accepted 25 Apr 2008; published 6 May 2008

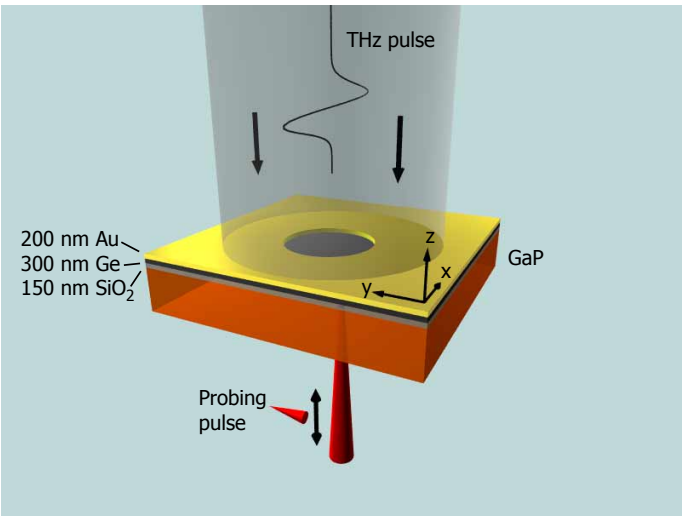

Fig. 1. Detail of the experimental setup to measure the *z*-component of the near-field of a hole. The electric field of a THz pulse is incident on the hole. The local electric field E_z is measured using the synchronized probe laser pulse (red). A highly reflective combination of a Germanium (Ge) and a SiO_2 layer, prevents the probe from reflecting off the gold layer.

cited analytical approximation of the near-field of a small hole is the model of Bethe which was later improved by Bouwkamp.[14, 15, 16] An uncomfortable aspect of the Bouwkamp model, which is based on a perfectly conducting, infinitely thin metal, is that the charge accumulation at the edges of the hole produces a singularity in the electric field, which cannot occur for a real, physical hole. Similar problems can arise in Finite Difference Time Domain (FDTD) numerical calculations around sharp edges. There have been numerous reports on *far-field* measurements of light transmitted by both bare and structured single holes, especially in the THz frequency range.[17, 18]. It is essential to understand that far-field measurements cannot provide the required information on the near-field either. This is because in the far-field, much information about the near-field, such as the presence of evanescent waves, or the spatial distribution of the surface charge density, is inevitably lost. Therefore, to understand the behavior of light near a small hole, it is essential to *measure* the electric near-field of the hole directly.

Here, we show near-field measurements of small, individual holes in the THz frequency domain, using the technique of terahertz time-domain spectroscopy (THz-TDS).[19] This technique enables us to measure the time-dependent *electric near-field* component perpendicular to the metal, $E_z(t)$, in the vicinity of the hole in an ultra-broad bandwidth. It has a deep sub-wavelength spatial resolution of about 10 μm, which corresponds to a vacuum-wavelength related spatial resolution of $\lambda/300$, for $\lambda = 3$ mm. As we will show below, the broad bandwidth, which covers more than a decade in frequency from 0.1 to 1.2 THz, allows us to measure the near-field of the hole for incident THz wavevectors *k* for which $ka \ll 1$, and $ka \approx 1$, with *a* the radius of the hole.

Key to measuring the electric near-field around the hole with a high spatial resolution, is the direct placement of the hole on the surface of a THz field-sensitive detector, which consists of a GaP electro-optic crystal on which the metal, a 200 nm thick gold layer with a hole, is deposited. A single-cycle, broadband THz pulse[20] is incident on the hole. In the (001) oriented crystal, the *z*-component of the electric field is electro-optically measured using a synchronized,

#94461 - $15.00 USD Received 1 Apr 2008; revised 25 Apr 2008; accepted 25 Apr 2008; published 6 May 2008

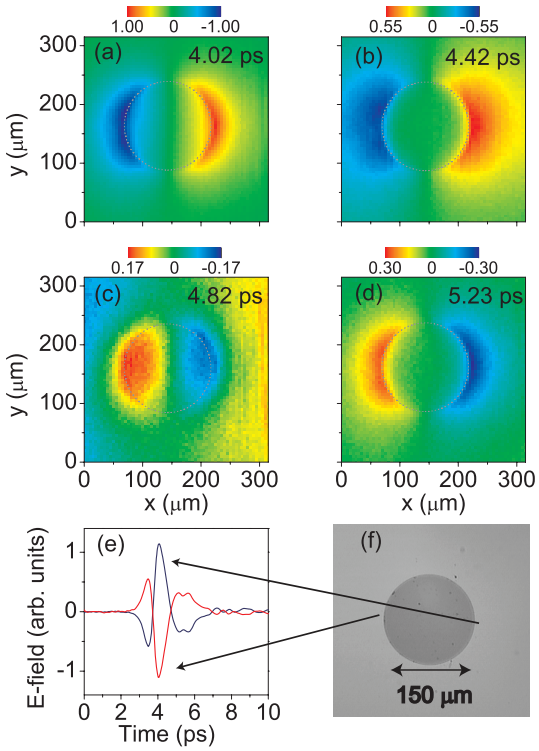

Fig. 2. (a)-(d) Two-dimensional maps of the THz near-electric field component E_z, measured near a 150 μm diameter hole in a 200 nm thick gold film, for four different times indicated in the figures. Scale bars show the relative strength of the measured fields. Blue indicates negative electric fields, red indicates positive electric fields. The dashed circles indicate the circumference of the hole. A movie showing the field at intermediate times is shown online (3.9 Mbyte)(e) Time dependent electric field transients measured at the edges of the hole at the locations indicated in the photograph of the hole shown in (f).

femtosecond probe laser pulse which is focused to an approximately 5μm diameter spot near the hole (Fig. 1).[21, 22] The use of the (001) oriented crystal guarantees that the setup is blind to the x and y components of the electric field. The crystal with the sample is raster-scanned in the xy-plane and at each position (x,y), a full 20 ps long THz electric field trace is measured. From $E_z(x,y,t)$, snapshots of the spatial distribution of the field at different times are produced, and from the Fourier transform $E_z(x,y,\omega)$, the spatial distribution of the various frequencies within the bandwidth of the THz pulse can be determined. The hole diameters used in our experiment are 100, 150 and 200 μm. The vacuum wavelengths of the near-field components that we can comfortably measure, range from 250 μm to 3 mm. To put this in perspective, a comparable measurement performed in the visible part of the EM spectrum on a 200 nm diameter hole, would require a measurement of the electric field of an approximately 1 fs long, single-cycle pulse with a temporal resolution of 100 attoseconds, in a bandwidth from 250 nm to 3000 nm, which, at present, is not feasible. In Fig. 2(a-d), we plot the z-component of the electric field, measured underneath a 150 μm diameter hole, at four different times during the emergence of the THz pulse through the hole. A movie showing intermediate times is shown online (3.5 Mbyte). The incident field is polarized in the x direction. Note that in the frames (a-d), the color scales are individually matched to the maximum amplitude range of each frame.

#94461 - $15.00 USD Received 1 Apr 2008; revised 25 Apr 2008; accepted 25 Apr 2008; published 6 May 2008

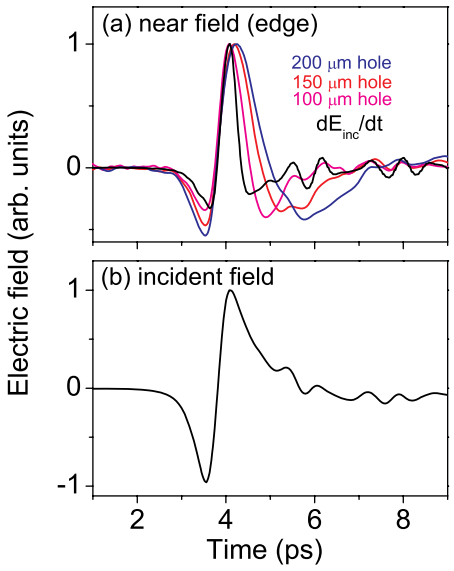

Fig. 3. Comparison between the measured electric field of the incident pulse (b), the calculated time-derivative of the field of the incident pulse and the measured near electric fields (a). The figure shows that as hole size decreases, the measured near-field at the edge increasingly resembles the time-differentiated incident electric field.

The images in Fig. 2(a-d) show that directly underneath the hole, only a weak E_z component is observed. At the edges of the hole, however, $|E_z|$ dramatically increases. Fields from opposite sides of the hole along the *x*-axis, are opposite in sign. This can also be seen from Fig. 2(e), where we plot two examples of the THz electric field as a function of time, measured at two locations close to the edge at opposite sides of the hole, as shown in the photograph of the hole in Fig. 2(f). The strength of the field, following a circular path along the edge of the hole, is not constant, however, but follows a $\cos(\phi)$-like dependence. We emphasize that the time-dependent near-fields measured at the edges, as shown in Fig. 2(e), are different from the unperturbed electric field incident at the hole. In fact, our measurements strongly suggest that in the time-domain, for decreasing hole size, the measured electric near-field increasingly resembles the time-differentiated incident electric field. This is shown in Fig. 3(a), where we plot the near electric-field transients measured at the edge of the 100, 150, and 200 μm diameter holes, together with the time-differentiated incident electric-field transient. For comparison, Fig. 3(b) shows the incident electric-field transient. This will be discussed in more detail below.

In total, the four frames cover a time window of 1.2 ps. Already, they give us an intuitive understanding of the time evolution of the THz electric field as it emerges from the sub-wavelength hole. Similar results are obtained for a square hole, as shown in Fig. 4. There, the raster-scanned area is large enough to observe the formation of a spherical wave propagating outwards from the hole as time progresses. Note that in frames (a) and (c), a small feature is visible near the top of the frames. Inspection of this sample using a microscope revealed that at that location the gold film was damaged, giving rise to an irregularly shaped, 20x40 μm^2, hole. Analysis of the measured data shows that the field transmitted by this hole contains mostly higher frequency

#94461 - $15.00 USD Received 1 Apr 2008; revised 25 Apr 2008; accepted 25 Apr 2008; published 6 May 2008

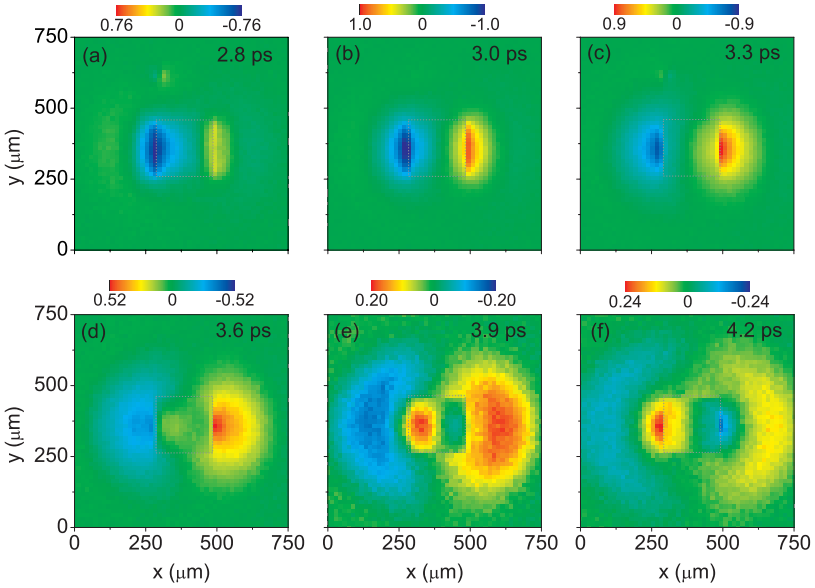

Fig. 4. (a)-(f) Two-dimensional maps of the THz near-electric field component E_z, measured near a 200x200 μm^2 square hole in a 200 nm thick gold film on GaP, for six different times indicated in the figures. Scale bars show the relative strength of the measured fields. Blue indicates negative electric fields, red indicates positive electric fields. The dashed squares outline the edges of the square hole. The fairly large size of the scanned area, makes it possible to see the formation of a spherical wave propagating outwards from the hole.

components. The advantage of measuring the near-electric field instead of the optical power becomes clear when we consider the boundary conditions for the perpendicular component of the electric field E_z at the metal-dielectric interface. These conditions state that this component is discontinuous across the metal-dielectric interface, with an amount determined by the surface charge density σ, giving $\sigma = E_z/\varepsilon$. This means that the two-dimensional, time-dependent, field plots shown in Fig. 2, can also be interpreted as two-dimensional maps of the surface charge density $\sigma(x,y,t)$, a quantity that cannot be obtained from a measurement of the optical *power*. We caution, however, that this is approximately true only, since our detection technique does not measure the field exclusively at the surface of the metal, but also at some distance away from it. This explains why in Fig. 2(c), at t=4.82ps, when the field right at the edge has just changed sign and has a value close to zero, the maximum field strength is observed directly under the aperture, where there's no metal and no surface charge density should be present.

The broad bandwidth of our THz pulses allows us to determine the frequency-dependent near-field transmission characteristics of the holes over a very large frequency range. As an example, we plot in Fig. 5(a), the measured two-dimensional distribution of the amplitude, $|E_z(x,y,\omega)|$, at a frequency of $\omega/2\pi = 0.2$ THz, acquired directly underneath the 150 μm diameter hole. 0.2 THz corresponds to a free space wavelength of 1.5 mm and to a wavelength of 455 μm inside the GaP electro-optic crystal, which is considerably larger than the diameter of the hole. The figure clearly shows that the field is strongly localized near the edge of the hole

#94461 - $15.00 USD Received 1 Apr 2008; revised 25 Apr 2008; accepted 25 Apr 2008; published 6 May 2008

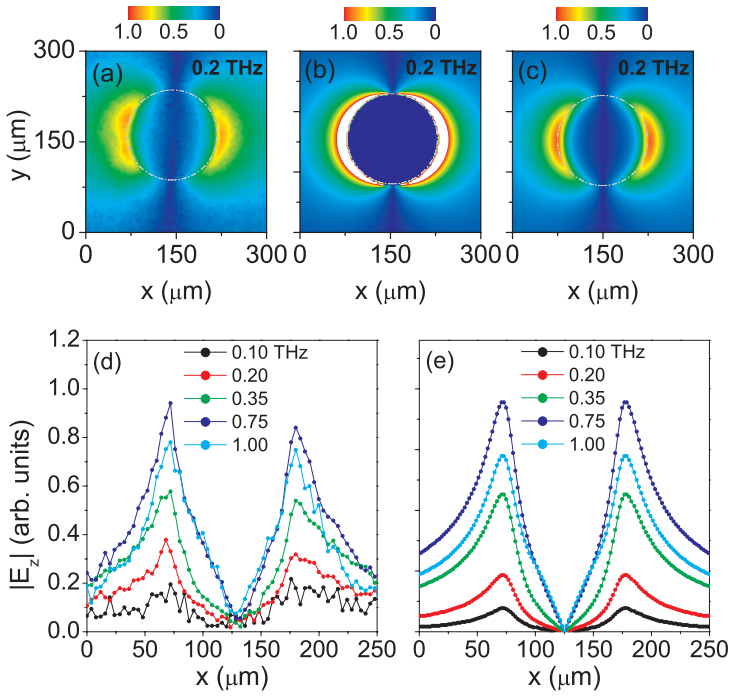

Fig. 5. (a) Measured spatial distribution of the z-component $|E_z|$ of the electric field behind a 150 μm hole in a 200 nm thick gold film deposited on a GaP electro-optic crystal, at 0.2 THz. The dashed circle indicate the circumference of the hole. (b) Spatial distribution of $|E_z|$, calculated using the Bouwkamp model. White indicates electric field values higher than the range of values indicated by the scale bar. (c) Spatial distribution of $|E_z|$ at a height of 10 μm above the metal, obtained using FDTD calculations. (d) Electric field $|E_z$, measured along the line y =152 μm, across a 100 μm diameter hole, for different frequencies. (e) FDTD calculations of the field along a line through the center of the 100 μm hole, at z =10 μm.

in the direction of the incident field, with an amplitude that strongly depends on the azimuthal angle ϕ. In Bouwkamp's model for the diffraction of light by a sub-wavelength hole, the near-field z-component of the electric field of a hole at the shadow side of an infinitely thin, perfectly conducting metal, at $z = 0$ is written as:

$$E_z = E_0 \frac{4i}{3} ka \frac{a/\rho}{\sqrt{\rho^2/a^2 - 1}} \cos(\phi), \qquad (\rho > a) \tag{1}$$

with a the radius of the hole, ρ the radial coordinate, ϕ the azimuthal angle, E_0 the electric field amplitude and k the wavevector of the incident radiation. In Fig. 5(b), we plot the $E_z(\rho, \phi)$ thus calculated. To show the $\cos(\phi)$ dependence, while at the same time avoiding problems related to the unphysical infinite field strengths predicted by the model at the edge when $\rho \to a$, we only plot the calculated field values lower than a certain value, arbitrarily chosen to facilitate a comparison with the measured data. Higher field values are given the color white. A comparison between the measurement and the calculations clearly shows that the $\cos(\phi)$ dependence predicted by the model, is indeed observed in the measurements. Note that the Bouwkamp model was derived under the condition that the metal layer is embedded in a continuous isotropic dielectric medium. Although this is strictly speaking not the case in our experiment, the exper-

#94461 - $15.00 USD Received 1 Apr 2008; revised 25 Apr 2008; accepted 25 Apr 2008; published 6 May 2008

imentally observed $\cos(\phi)$ dependence suggests that the GaP crystal has little effect on the azimuthal angle dependence predicted by the model. For comparison, we also performed FDTD calculations of the near-field amplitude at 0.2 THz, taking the dielectric constant of the GaP substrate into account. In our FDTD simulations, a single circular hole of 150 micron diameter, in a perfect conductor, was used. A metal layer of 6 μm was used. Thinner metal layers could not be used since they require unacceptable long calculation times. A plane-wave was used as the incident wave, and we attached a perfectly matched layer (PML) below the GaP crystal of 300 micron to completely absorb light which in the calculations makes the crystal effectively infinitely thick. The mesh width was chosen to be 2 micron. The refractive index of the crystal was set to be 3.19. As in the Bouwkamp model, FDTD calculations predict infinitely large field strengths at an infinitely sharp edge. Good agreement with the experimentally observed 2D distribution is found when the field is calculated at a distance of 10 μm away from the surface (Fig. 5(c)). This calculation confirms that our measurement technique samples the electric near-field close to the metal surface at a distance which is orders of magnitude smaller than the wavelength.

To further illustrate the frequency dependence of the field, we plot in Fig. 5(d) the electric field $|E_z|$ along the line $y = 152$ μm in the direction of the incident field polarization, underneath a 100 μm diameter hole, for a number of different frequencies from 0.1 THz to 1 THz. The curves for each frequency are divided by the amplitude of the corresponding frequency in the spectrum of the incident pulse, to compensate for the non-flat spectrum of the incident pulse. At all frequencies, the curves plotted in Fig. 5(d) show maxima around the edges of the hole. Surprisingly, whereas the amplitude increases when the frequency increases to about 0.75 THz, it drops to a lower value again at a frequency of 1 THz. The same behavior is observed in FDTD calculations performed in a plane 10 microns below the metal, which are in excellent agreement with the measured results as shown in Fig. 5(e).

To confirm the frequency-dependence of the near-field amplitude, we plot in Fig. 6 the frequency-dependent electric near-field amplitude E_z, measured at the edge, for the three different hole diameters used in our experiments. Again, the signals are divided by the spectrum of the incident THz pulse to facilitate an absolute comparison between the amplitudes at the different frequencies. For the 100, 150 and 200 μm diameter hole, maxima in the field measured at the edge are observed at about 0.6, 0.4 and 0.3 THz respectively. At higher frequencies, the electric field for all three holes reaches values which are the same to within the measurement accuracy at these frequencies. The maxima observed in Fig. 6, are located close to the cut-off frequency of the lowest order mode of a circular waveguide, the TE_{11} mode, if we assume that hole is located inside a dielectric medium with the refractive-index of GaP, n=3.3. This is consistent with the recently observed microwave far-field transmission enhancement of holes caused by filling the holes with a dielectric material.[23] Our results also resemble the peak transmission obtained in single hole transmission experiments reported at visible/near-infrared wavelengths.[8] There, however, plasmon and skin depth effects make it more difficult to establish a connection between the cut-off frequency and the frequency where the maximum transmission occurs.[24] Here, we calculate cut-off frequencies of 0.54, 0.35 and 0.27 THz for holes of 100, 150 and 200 μm respectively, which is very close to the observed frequencies where the maxima occur. Although the results for the three holes look very different, they qualitatively agree with the predictions made by García de Abajo for the enhancement of the transmission cross-section (normalized to the hole area) near the cut-off frequency of a hole in a perfect metal (see Fig. 7).[25] However, this agreement doesn't necessarily prove that the maxima observed here have the same physical origin as the calculated enhanced transmission cross-section. The maximum in the near-field measured at the metal edge could also be the result of an increased angular diffraction when the frequency decreases to the cut-off frequency

#94461 - $15.00 USD Received 1 Apr 2008; revised 25 Apr 2008; accepted 25 Apr 2008; published 6 May 2008

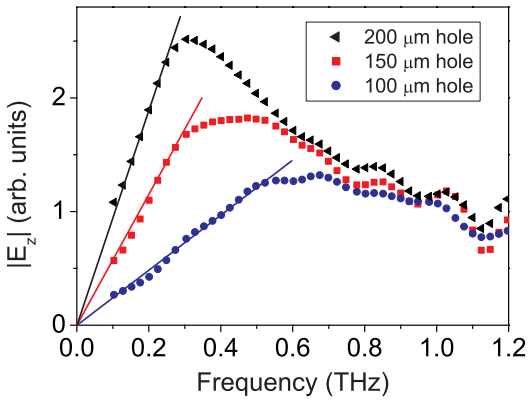

Fig. 6. Measured electric field at the edge of the hole as a function of frequency, for hole diameters of 100, 150, and 200 μm. The spectra are divided by the spectrum of the incident THz pulse. The straight lines originating from the origin are guides to the eye.

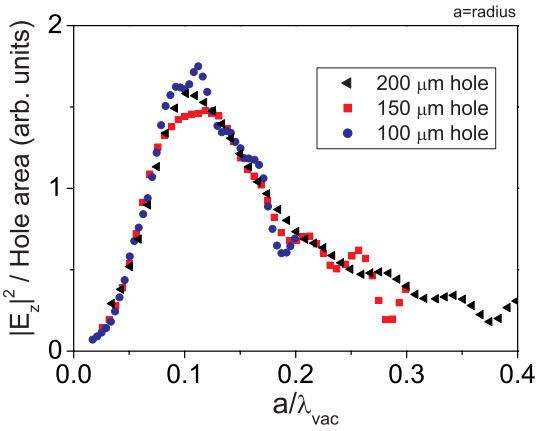

Fig. 7. Normalized and scaled version of Fig. 4 to allow a comparison with the paper by Garcia de Abajo.[25] To within measurement signal-to-noise, the curves are identical, which is a manifestation of the scale-invariance of Maxwell's equations at THz frequencies, where the perfect conductor approximation is a valid assumption.

#94461 - $15.00 USD Received 1 Apr 2008; revised 25 Apr 2008; accepted 25 Apr 2008; published 6 May 2008

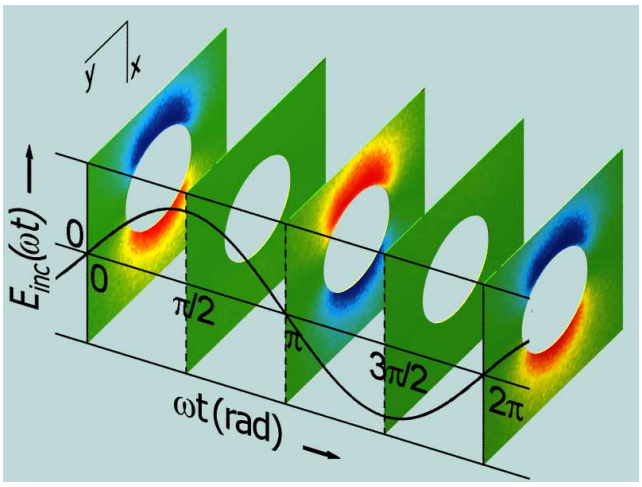

Fig. 8. Electric near-field E_z around a hole, at 5 times during a single period of a sinusoidal incident electric field (black curve) with a frequency of 0.2 THz, showing maximum near-field amplitudes during a zero-crossing of the incident electric field, and zero near-field strength during a maximum of the incident electric field. Blue and red indicate positive and negative E_z respectively. The 2D near-field distributions were obtained from a Fourier analysis of the measured electric near-field pulse. Note that the phase-shift between the incident field and the near-field is implied by our measurements even though our setup can currently not measure the absolute phase difference between the incident electric field and the electric near-field.

of the holes.

We now concentrate on the portion of the curves in Fig. 6 below the cut-off frequencies. In this frequency range, the amplitude clearly increases linearly with frequency, which can be seen by comparison with the straight lines that we plotted in Fig. 6 as guides to the eye. This agrees with Bouwkamp's model, eq. (1), which predicts that the field amplitude increases linearly with k and thus with ω. It also agrees with our earlier observation that the measured near-field increasingly resembles the time-differentiated incident field for smaller apertures. The frequency analysis shows that the linear part (for $ka \ll 1$), where $E_z(\omega) \propto \omega$ and thus $E_z(t) \propto dE_{incident}/dt$, covers a larger frequency range when the hole size decreases. Thus, when the hole size decreases, and more and more wavelengths in the bandwidth of the incident pulse obey $ka \ll 1$, the corresponding frequencies fall into this linear regime, making the approximation $E_z(t) \propto dE_{incident}/dt$ in the time-domain, increasingly accurate. Even though our setup cannot measure the phase-difference between the incident electric field and the near-field, our analysis implies that the near-field must be $\pi/2$ out of phase with the incident electric field for frequencies much lower than the cut-off frequency. This means that for an incident sinusoidal electric field, the near-field reaches a maximum when the incident field goes through a zero crossing, as illustrated in Fig. 8 for a frequency of 0.2 THz.

We would like to point out that in contrast to our near-field measurements, *far-field* hole *power* transmission experiments tentatively show a ω^6 dependence.[26, 27, 28] This once again emphasizes the difference between the properties of the near-field and the far-field and underlines the importance of performing near-field experiments.

One advantage of performing the experiments at THz frequencies instead of at visible frequencies, is related to the larger size of the structures on which the experiments are performed. Holes of 100 to 200 μm diameter are just visible to the naked eye, and are fairly easy to

#94461 - $15.00 USD Received 1 Apr 2008; revised 25 Apr 2008; accepted 25 Apr 2008; published 6 May 2008

make. This scaling advantage, however, is not limited to the THz frequency range and one can speculate whether similar near-field experiments on holes at microwave- or even radio-wave frequencies haven't already been published, just as the first applications of extraordinary optical transmission of hole arrays were already published in 1952.[29] However, although near-field experiments have been performed on metal half-planes[30] and slits[31], we have been unable to find comparable, published, experiments on holes. We therefore conclude that our experiments are the first to show the detailed time and broadband frequency dependence of the electric near-field of sub-wavelength sized holes.

2. Conclusion

The measured time- and frequency-dependence of the THz near-electric field of a single hole provides us with a detailed understanding of the behavior of light near sub-wavelength structures. Not only is this relevant for near-field micro-spectroscopy, but we also anticipate that this information can be used for strategies to increase the local field strength of specially designed holes for non-linear optical applications, such as edge-enhanced Raman scattering and infrared near-field microscopy. Since micro fabrication is very simple, the presented THz approach also appears to be very attractive as an experimental platform for sub-wavelength structures intended for an application in the optical domain.

#94461 - $15.00 USD Received 1 Apr 2008; revised 25 Apr 2008; accepted 25 Apr 2008; published 6 May 2008